Air-rail timetable synchronization: Improving passenger connections in Europe within and across transportation modes

Clara Buire, Aude Marzuoli, Daniel Delahaye, Marcel Mongeau

Air-rail timetable synchronization: Improving passenger connections in Europe within and across transportation modes

Clara Buire, Daniel Delahaye, Marcel Mongeau
ENAC, Université de Toulouse,
Toulouse,
France,
firstname.surname@enac.fr

Aude Marzuoli,
Georgia Institute of Technology,
North Ave NW, Atlanta, GA
United-States
aude.marzuoli@gmail.com

Abstract

This study addresses the integration of the railway and airline scheduling problems, in order to offer passengers smooth transfers between rail and air. This paper focuses on optimizing the air and rail timetables at 18 major European airports including three hubs and their associated train stations. A multimodal passenger demand simulation, using constraint programming and based on real data, is proposed. Six days in December 2019 are analyzed, and ten simulations per day are performed. These instances are publicly released. The air-rail timetable synchronization is applied to these 60 simulated days. Three scenarios are tested in which each operator agrees to change its schedule or not. Results show that changing only 13% of European flights by 11 minutes on average could increase the number of suitable connections for passengers by 60%. In addition, if both airlines and railway operators adapt their schedules, passenger comfort is improved and operator costs are reduced, even more so than with unilateral changes.

Keywords— Air-rail integrated timetable, optimization, passengers, multimodal demand, Mixed-Integer Linear Programming, Constraint Programming

1 Introduction

By 2050, the European Commission plans to build a resilient long-distance European multimodal network, in which passengers can "transfer seamlessly between modes" (European Commission [2011a,b]). They define several goals such as 90% of passengers within Europe are able to complete their door-to-door journey in less than four hours. To support this objective, the European Commission emphasizes the need for a better integration of the air transportation system particularly with ground transportation modes, such as rail. At the same time, airport capacity congestion and increasing environmental awareness make rail transportation a relevant alternative to short-haul flights. For instance, in 2021, the French government voted a law with the purpose of replacing short-haul flights by trains. However, to maintain attractiveness and limit passengers discomfort of shifting between modes, collaboration between air and rail will be required. To promote this goal, Europe launched several research projects such as TRANSIT (Bueno et al. [2022]) or MODUS (Paul [2020]) to measure the improvement in terms of air and rail connectivity. The former project establishes that a collaborative decision making process between air and ground transportation modes could benefit passengers in terms of seamless transfer and during disruptions. MODUS project highlights that data sharing, passenger-centric system and knowledge about passenger demand are keys to develop a resilient door-to-door transportation system.

In this study, we propose to refine flight and rail schedules to promote the quality of passenger multimodal transfers at hub airports. The objective consists in optimizing flight and train schedules, from a passenger perspective, to offer passengers seamless connection in terms of transfer times. The study considers a set of airports and train stations, and network effects are modeled, since changing the departure time of a flight or a train at its origin station is likely to affect its arrival time at its destination. In addition, operational constraints such as airport and train station capacities and the preservation of air-air connections are considered. The contributions of this paper are the following. First, a

Mixed-Integer Linear Programming (MILP) formulation of the Air-Rail Timetable Synchronization (ARTS) problem at the network level is proposed. Then, in order to tackle the lack of publicly available data regarding air-rail multimodal demand, a generic method to simulate such demand is proposed. The generated instances are based on realistic data and publicly released. Finally, potential benefits of such a collaboration are quantified on three major European airports: Paris-Charles de Gaulle, Frankfurt and Madrid-Barajas airports. We show that if both airlines and railway operators agree to adapt slightly their schedules, the risk of missed connection for passengers could be reduced by 25% while reducing the average passenger waiting time at the airport. Results also reveal that bilateral changes would allow operators to share the cost of deviating their schedules, with a higher benefit for passengers.

This paper is organized as follows. Section 2 presents previous works related to air and rail integration. Then, the ARTS problem and the associated mathematical formulation are introduced in Section 3. In Section 4, a generic method to simulate an air-rail passenger demand is detailed. Finally, Section 5 presents results obtained on the Western European case study, followed by concluding remarks.

2 Previous related works

Air and rail operators have been traditionally viewed as competitors (D'Alfonso et al. [2016, 2015]). However, with increased airport congestion and growing environmental awareness, air and rail cooperation has received a growing interest in recent years. Indeed, Givoni and Banister [2006] show that replacing short-haul flights by trains could relieve airport congestion. Jiang and Zhang [2014] highlight that air-rail collaboration would benefit for both operators and passengers, especially when hub airports are facing capacity constraints. Janic [2011] studies the effect of transforming a large airport into a multimodal platform on passengers and environment. The author states that replacing short-haul flights by High-Speed Rail (HSR) could reduce flight delays and passenger delays, noise and greenhouse gas emissions. Chiambaretto et al. [2013] study several air-rail intermodal services that could be offered to passengers, such as guarantee in case of delay or smooth connection time. For each service offered, the willingness to pay is estimated. Authors show that long connection times are not desired by passengers, especially for business travelers. Xia and Zhang [2017] study the effect of air-rail connecting time on both operators and passengers. They show that passengers would benefit from a cooperation between air and rail through reduced connecting times. However, authors state that the cost of reducing connection time should be fairly shared between airlines and railway operators to incentivize stakeholders to change their operations. Clewlow et al. [2012] explain that timetable coordination was implemented in Germany between Lufthansa and Deutsche Bahn on two rail segments in 2007, with the purpose of reducing transfer times between trains and flights on Cologne-Frankfurt and Stuttgart-Frankfurt segments. Most of these studies emphasize the need of air-rail schedule synchronization. Indeed, schedule synchronization is of major importance for transportation operators to maintain attractiveness when no direct transfer can be offered to passenger. Regarding air transportation, several metrics are proposed to assess the quality of flight schedule synchronization at hub airports (Burghouwt and Redondi [2013], Veldhuis [1997], Dennis [1994], Burghouwt and de Wit [2005], Danesi [2006]). Similarly, railway operators design their schedules in order to minimize passenger waiting time at transfer stations (Nachtigall and Voget [1996], Knoppers and Muller [1995], Jansen et al. [2002], Vansteenwegen and Van Oudheusden [2006]). Managing connecting time between rail and air services is thus a key lever to ensure a seamless multimodal transfer. However, few studies deal with the integration of the air and rail timetables, especially at a large scale. Ke et al. [2020] propose a rail schedule optimization at Shijiazhuang Zhengding airport HSR station to maximize the number of feasible connections with departing flights. Jiang et al. [2022] include synchronization with flights in the intercity HSR scheduling problem. They ensure that a minimum number of trains is available for each landing flight at the airport. Buire et al. [2022] deal with synchronizing flight and HSR schedules at Paris-Charles de Gaulle airport to provide passengers with smooth connections. These studies mainly focus on synchronizing rail and air schedules between one airport and one train station. However, changing the schedule at one station is likely to change the schedule in the overall transportation network. In this paper, we therefore propose to address the air-rail timetable synchronization problem at the multimodal network scale. As in Buire et al. [2022], limited changes are authorized to minimize the impact on transportation operators schedule. In addition, air-air connections are guaranteed. We first simulate a realistic passenger demand, from origin cities to destination cities, leveraging real transportation data. We then solve the ARTS problem using that demand. The ARTS problem formulation is presented in the next section.

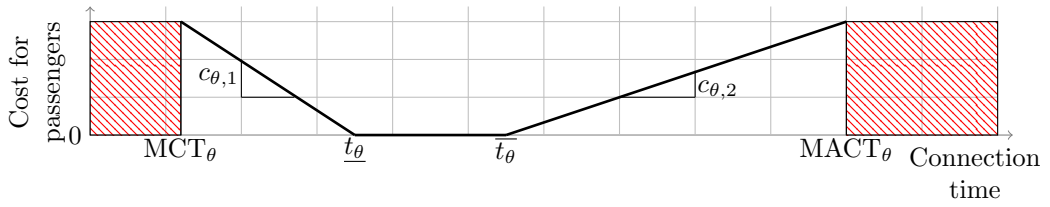

Figure 1: Passenger discomfort cost c_θ for a connection type θ as a function of connection time.

3 Problem statement, mathematical formulation and resolution approach

The objective of the study is to generate an integrated timetable between air and rail that provides passengers with smooth connections. In this section, the passenger comfort assessment is first introduced. Then, a mathematical formulation of the timetable synchronization problem is proposed and a resolution approach is detailed. In the sequel, a flight or a train is referred to as a *leg*.

3.1 Assessing the passenger transfer time

When passengers travel, they can make direct connections between their origin and destination if there is a direct flight or train. Otherwise, they have to transfer between two legs within the same network (*intramodal* connection) or they can shift to another mode (*intermodal* connection). In order to make a transfer feasible, a minimum transfer time between legs is necessary for passengers. This time should include the transfer time between the two stations in case of multimodal connection (if the airport is not directly linked with an HSR station for instance), and eventually a station processing time (check-in, security screening at airport, border controls, luggage collection after a flight, etc.). In the following, MCT denotes this minimum connection time, the minimum time required to transfer between two legs when no disruption occurs during the transferring process (e.g., queuing at check-in or security screening). Similarly, MACT denotes the maximum acceptable transfer time for passengers. Above the MACT limit, we assume that passengers do not choose the connection (too large waiting time). We propose to assess the transfer time between two legs by refining the model proposed in Buire et al. [2022]. Instead of limiting the ideal transfer time to a unique value, we define a time interval $[\underline{t},\overline{t}]$ that contains transfer durations that are considered as ideal for passengers. The values chosen MCT, MACT, $\underline{t}$ and $\overline{t}$ may depend on the connection type considered. This allows one to take into account a longer transfer time, for example, for passengers catching a flight with an international destination, or when the train station is not directly at the airport. In the sequel, we denote Θ the index set of connection types (from a train to a domestic flight, from a train to a non-domestic flight, from flight to flight, etc.), and MCT_θ, MACT_θ, $\underline{t_\theta}$ and $\overline{t_\theta}$, will denote the parameters defined for connection type θ, $\theta \in \Theta$. To measure the quality of a transfer duration, we introduce a piecewise-linear function, c_θ, of the connection time, t, between the two legs that directly results from the train and flight timetables. For the sake of simplification, we consider in this study a function with only two breakpoints, $\underline{t_\theta}$ and $\overline{t_\theta}$, as illustrated by Figure 1. One can however easily adapt the model with a function featuring additional breakpoints as this does not affect the computational complexity of our model. We assume that short connection times are less desirable than long connection times. Indeed, short connections are not robust for passengers in case of delay. Passengers are likely to prefer connections with an additional buffer time to limit the risk of missed connections. Consequently, the unit cost of short connection times is assumed to be higher than long ones. The explicit formula for the passenger discomfort cost function is the following one:

$$c_\theta(t) = \begin{cases} c_{\theta,1}t + b_{\theta,1} & \text{MCT}_\theta \leq t \leq \underline{t_\theta} \\ c_{\theta,2}t + b_{\theta,2} & \overline{t_\theta} \leq t \leq \text{MACT}_\theta \\ 0 & \text{otherwise.} \end{cases} \tag{1}$$

As the connection time between two legs gets closer to the ideal interval $[\underline{t_\theta}, \overline{t_\theta}]$, the cost of the connection decreases linearly toward 0. The cost of a connection with an ideal connection time, more precisely if the transfer time is within interval $[\underline{t_\theta},\overline{t_\theta}]$, equals 0. The objective of the air-rail timetable synchronization problem is to adjust timetables in order to ensure smooth transfer for passengers. In other words, create an integrated timetable with transfer times ranging between MCT_θ and MACT_θ, and with the lowest cost, c_θ, for each passenger having a connection of type $\theta \in \Theta$. We assume that connection times under MCT_θ and above MACT_θ are not allowed, however one can easily relax these constraints by adding a large unit cost when the connection time is beyond these two values.

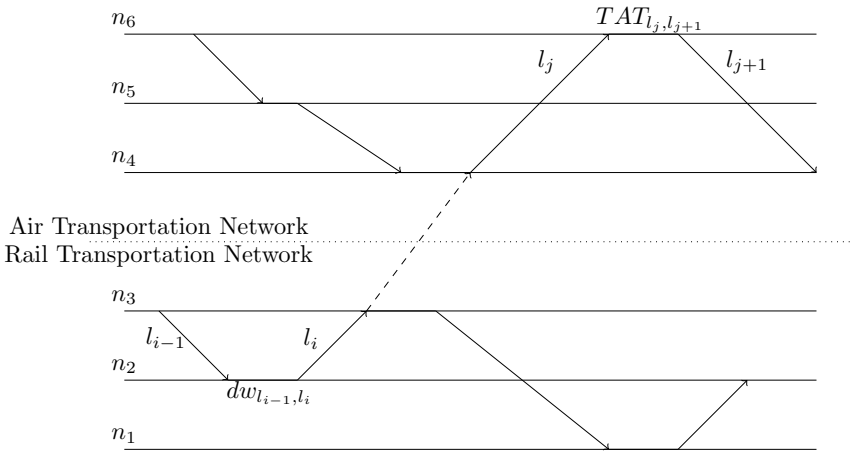

Figure 2: Time-expanded flight and rail-leg network. The dashed line illustrates a passenger transfer from a rail leg to a flight.

In this study, we assume that the problem is addressed several weeks before the day of operation. Several transportation operators constraints are considered. First, we propose an airport capacity model, in terms of number of scheduled arrivals and departures, limited to the airport current capacities. The number of trains stopped at each station cannot exceed the number of tracks. Then, a minimum aircraft turnaround time and a constant train stop time at station are taken into account. Finally, network effects are also modeled: the in-vehicle time is assumed to be fixed and the change in departure time of one leg at its origin station implies a change in its arrival time at destination. Input data, decision variables, constraints and the objective function of the proposed MILP formulation are presented below.

3.2 Optimization problem formulation

An entire day is considered from 12am to 12pm. For simplification purpose, only connections from a train to a flight are considered; however, the model can be easily generalized to several connection types.

3.2.1 Sets and parameters

In the following, index sets related to the air transportation network and index sets related to the rail transportation network will be super-scripted by "air" and "rail", respectively. The index set of stations of the considered network, noted $\mathcal{N}$, is partitioned into the airport index set, $\mathcal{N}^{\text{air}}$, and train station index set, $\mathcal{N}^{\text{rail}}$. During a day of operations, flights are operated by aircraft and rail legs by trains. We denote $\mathcal{L}$ the index set of legs partitioned into the flight index set, $\mathcal{L}^{\text{air}}$, and the rail-leg index set, $\mathcal{L}^{\text{rail}}$. Let $\mathcal{P}^{\text{air}}$ and $\mathcal{P}^{\text{rail}}$ be the index set of flight pairs and rail-leg pairs operated consecutively by the same vehicle. An operational day can be represented by a time-expanded network, as illustrated for one train and one aircraft in Figure 2. For each station $n \in \mathcal{N}$, we define $\mathcal{L}_n^A$ and $\mathcal{L}_n^D$ the index set of the legs arriving at station n and departing from station n, respectively.

Travelers can use one or more services (rail legs and flights) to reach their final destination. If there is no direct leg, they have to transfer between two legs. For instance, a passenger transfer between a train and a flight is represented by the dashed line in Figure 2. A transfer corresponds to a link between two legs l_i and l_j, $(l_i, l_j) \in \mathcal{L} \times \mathcal{L}$. We denote $\mathcal{E}$ the index set of passenger connections. A passenger connection $e \in \mathcal{E}$ is detailed as $e = (l, l', d_e, \theta_e) \in \mathcal{L} \times \mathcal{L} \times \mathbb{N} \times \Theta$, where l and l' are the first leg and second leg, respectively; d_e is the passenger volume demand for that connection and θ_e the connection type. This formulation allows one to consider both intermodal and intramodal connections. In our study, we aim at improving connections for passengers transferring from a train to a flight, while maintaining connectivity for air transferring passengers. Thus, the index set of passenger connections, $\mathcal{E}$, is partitioned into the index sets $\mathcal{E}^{\text{rail,air}}$, which refers to multimodal passengers, and $\mathcal{E}^{\text{air,air}}$ for air transferring passengers. Since transfer times between stations are taken into account, we denote $\pi_{l,l'}$ the transfer time between the arrival station of leg l and the departure station of leg l', $(l, l') \in \mathcal{L} \times \mathcal{L}$. If transfers occur within the same station, or if the train station is located at the airport, the transfer time between the airport and the train station is assumed to be 0. Note that in practice, depending on the airport configuration, it may in fact require some times for passengers to reach their

departure terminal from the train station, even if it is directly located at the airport. This parameter can be set by the final user to a value different from 0.

Discrete time intervals of h minutes are considered. We set h to 5 minutes in this study. An interval time is denoted a slot, hence $N_{\text{slots}} = 288$ slots are defined (a 24-hour day is considered). Then, airport runway capacities are evaluated to limit airport congestion. More precisely, the number of arriving flights that could be scheduled within a given time window is limited, and similarly for departing flights. In common practice, these capacities are set for 10- and 60-minute intervals (Cohor [2023], Fluko [2023]), and these capacities depend on the time of the day (a higher capacity is allowed during peak hours). Both duration intervals will be considered in the optimization problem. We denote W the set of possible durations (slot windows) on which the airport runway capacities are evaluated. In order to guarantee air-air connections, a maximum deviation of Δ minutes is allowed compared with the initial connection time. Finally, in order not to perturb significantly the operators' schedules, we set $\delta^{\max}$ the maximum deviation allowed assigned to each departure and arrival time in the schedule.

3.2.2 Input data

For each airport $n \in \mathcal{N}^{\text{air}}$, the maximal runway arrival and departure capacities per slot-window w are known (given input data). The set W is chosen so that, for each $w \in W$, $\frac{N_{slots}}{w}$ is an integer. As these values depend on the hour of the day, for each $w \in W$, and each slot $s \in \{0, 1, \ldots, \frac{N_{\text{slots}}}{w} - 1\}$, we denote $y_n^{A,w,s}$ and $y_n^{D,w,s}$, the maximum number of airport arrivals and departures that could be scheduled between slot sw and slot $(s+1)w - 1$. For each train station $n \in \mathcal{N}^{\text{rail}}$, the initial number of trains o_n^0 stopped at the station and the number of available tracks $o_n^{\max}$ are given. For each leg $l \in \mathcal{L}$, we denote $t_l^{A,0}$ the initial scheduled arrival time of l. Similarly, $t_l^{D,0}$ corresponds to the initial scheduled departure time of leg l, $l \in \mathcal{L}$. We denote, for each $l \in \mathcal{L}$, IVT_l, the in-vehicle time of leg l. For each pair of consecutive flights $(l, l') \in P^{\text{air}}$ operated by the same aircraft, we set $TAT_{l,l'}$ the minimum turnaround time at the airport between the two flights. We consider the initial turnaround time planned by airlines. Similarly, for each consecutive rail-leg pair $(l, l') \in P^{\text{rail}}$ operated by the same train, we denote $dw_{l,l'}$ the dwell time at the train station between leg l and l'. This time corresponds to the initial-schedule stop duration of the train between two legs, in order to drop-off some passengers and pick-up others.

3.2.3 Decision variables

Decision variables of the ARTS problem are defined as follows. For each leg $l \in \mathcal{L}$, we define the discrete decision variable, k_l^D, the index of the slot at which l is scheduled to depart. From this primary decision variable, several auxiliary optimization variables are defined. First, for each $l \in \mathcal{L}$, we set k_l^A the index of the slot at which l is scheduled to arrive. The discrete variables t_l^A and t_l^D are the new scheduled arrival time and departure time of l, $l \in \mathcal{L}$. From these variables, we define the discrete decision variable δ_l, the schedule deviation from the initial departure time of l, $l \in \mathcal{L}$. For each slot $s \in \{0, 1, \ldots, N_{\text{slots}}\}$, and each leg l, $l \in \mathcal{L}$, we denote $x_{l,s}^D$ and $x_{l,s}^A$, binary decision variables indicating respectively whether leg l is scheduled to depart after slot s, and scheduled to arrive after slot s, respectively. For each train station $n \in \mathcal{N}^{\text{rail}}$ and at each slot $s \in \{0, 1, \ldots, N_{\text{slots}}\}$, we define a discrete decision variable $o_{n,s}$ that counts the number of trains stopped at n at slot s. Finally, for each passenger connection $e \in \mathcal{E}^{\text{rail,air}}$, the continuous decision variable c_e denotes the passenger connection cost.

3.2.4 Optimization model

The objective is to generate a timetable between air and rail that minimizes the total multimodal passengers' transferring discomfort, while, as a secondary objective, keeping schedule deviation low. The optimization proposed is:

$$\min_{k,t,x,c,o} \sum_{e \in \mathcal{E}^{\text{rail,air}}} d_e c_e, \sum_{l \in \mathcal{L}} \delta_l, \tag{2}$$

$$k_l^A = k_l^D + \frac{IVT_l}{h} \qquad l \in \mathcal{L} \quad (2a)$$

$$t_l^D = h(k_l^D - 1) \qquad l \in \mathcal{L} \quad (2b)$$

$$t_l^A = h(k_l^A - 1) \qquad l \in \mathcal{L} \quad (2c)$$

$$t_l^D \leq t_l^{D,0} + \delta^{\max} \qquad l \in \mathcal{L} \quad (2d)$$

$$t_l^{D,0} - \delta^{\max} \leq t_l^D \qquad l \in \mathcal{L} \quad (2e)$$

$$t_l^D - t_l^{D,0} \leq \delta_l \qquad l \in \mathcal{L} \quad (2f)$$

$$t_l^{D,0} - t_l^D \leq \delta_l \qquad l \in \mathcal{L} \quad (2g)$$

$$TAT_{l',l} \leq t_{l'}^D - t_l^A \qquad (l,l') \in P^{\text{air}} \quad (2h)$$

$$dw_{l',l} = t_{l'}^D - t_l^A \qquad (l,l') \in P^{\text{rail}} \quad (2i)$$

$$k_l^D \leq s + M x_{l,s}^D \qquad l \in \mathcal{L}, s \in \{0,1,\ldots,N_{\text{slots}}\}, \quad (2j)$$

$$\sum_{s=0}^{N_{\text{slots}}} x_{l,s}^D \leq k_l^D \qquad l \in \mathcal{L}, \quad (2k)$$

$$k_l^A \leq s + M x_{l,s}^A \qquad l \in \mathcal{L}, s \in \{0,1,\ldots,N_{\text{slots}}\}, \quad (2l)$$

$$\sum_{s=0}^{N_{\text{slots}}} x_{l,s}^A \leq k_l^A \qquad l \in \mathcal{L}, \quad (2m)$$

$$\sum_{\tau=sw}^{(s+1)w-1} \sum_{l \in \mathcal{L}_n^A} x_{l,\tau}^A - x_{l,\tau+1}^A \leq y_n^{A,w,s} \qquad n \in \mathcal{N}^{\text{air}}, w \in W, s \in \{0,1,\ldots,\frac{N_{\text{slots}}}{w} - 1\}, \quad (2n)$$

$$\sum_{\tau=sw}^{(s+1)w-1} \sum_{l \in \mathcal{L}_n^D} x_{l,\tau}^D - x_{l,\tau+1}^D \leq y_n^{D,w,s} \qquad n \in \mathcal{N}^{\text{air}}, w \in W, s \in \{0,1,\ldots,\frac{N_{\text{slots}}}{w} - 1\}, \quad (2o)$$

$$o_{n,0} = o_n^0 \qquad n \in \mathcal{N}^{\text{rail}}, \quad (2p)$$

$$o_{n,s} = o_{n,s-1} + \sum_{l \in \mathcal{L}_n^A} (x_{l,s-1}^A - x_{l,s}^A) - \sum_{l \in \mathcal{L}_n^D} (x_{l,s-1}^D - x_{l,s}^D) \qquad n \in \mathcal{N}^{\text{rail}}, s \in \{1,2,\ldots,N_{\text{slots}}\}, \quad (2q)$$

$$o_{n,s} \leq o_n^{\max} \qquad n \in \mathcal{N}^{\text{rail}}, s \in \{0,1,2,\ldots,N_{\text{slots}}\}, \quad (2r)$$

$$t_{l'}^D - t_l^A - \pi_{l,l'} = t_1 + t_2 + t_3 \qquad e \in \mathcal{E}^{\text{rail,air}}, \quad (2s)$$

$$c_{\theta_e,1} t_1 + b_{\theta,1} + c_{\theta_e,2} t_3 \leq c_e \qquad e \in \mathcal{E}^{\text{rail,air}}, \quad (2t)$$

$$\text{MCT}_{\theta_e} \leq t_1 \leq \underline{t_{\theta_e}} \qquad e \in \mathcal{E}^{\text{rail,air}}, \quad (2u)$$

$$0 \leq t_2 \leq \overline{t_{\theta_e}} - \underline{t_{\theta_e}} \qquad e \in \mathcal{E}^{\text{rail,air}}, \quad (2v)$$

$$0 \leq t_3 \leq \text{MACT}_{\theta_e} - \overline{t_{\theta_e}} \qquad e \in \mathcal{E}^{\text{rail,air}}, \quad (2w)$$

$$t_{l'}^D - t_l^A \leq t_{l'}^{D,0} - t_l^{A,0} + \Delta \qquad e \in \mathcal{E}^{\text{air,air}}, \quad (2x)$$

$$t_{l'}^D - t_l^A \geq t_{l'}^{D,0} - t_l^{A,0} - \Delta \qquad e \in \mathcal{E}^{\text{air,air}}, \quad (2y)$$

$$t_{l'}^D - t_l^A \leq \text{MACT}_{\theta_e} \qquad e \in \mathcal{E}, \quad (2z)$$

$$t_{l'}^D - t_l^A \geq \text{MCT}_{\theta_e} \qquad e \in \mathcal{E}, \quad (2aa)$$

$$k_l^D, k_l^A \in \{1,2,\ldots,N_{\text{slots}}\} \qquad l \in \mathcal{L}, \quad (2ab)$$

$$t_l^A, t_l^D \in \{0,h,\ldots,h(N_{\text{slots}}-1)\} \qquad l \in \mathcal{L}, \quad (2ac)$$

$$\delta_l \in \{0,1,\ldots,\Delta\} \qquad l \in \mathcal{L}, \quad (2ad)$$

$$x_{l,s}^D, x_{l,s}^A \in \{0,1\} \qquad l \in \mathcal{L}, s \in \{0,1,\ldots,N_{\text{slots}}\}, \quad (2ae)$$

$$o_{n,s} \in \{0,1,\ldots,o_{n,s}^{\max}\} \qquad n \in \mathcal{N}^{\text{rail}}, s \in \{0,1,\ldots,N_{\text{slots}}\}, \quad (2af)$$

$$c_\theta \in [0,1] \qquad e \in \mathcal{E}^{\text{rail,air}}, \quad (2ag)$$

where M is some large-enough *big-M* constant to be set by the user. One can show that it is sufficient to set $M = N_{\text{slots}}$. We set M to this value in our study. Constraints (2a)-(2e) refer to the new schedule assignment and

to the maximum schedule deviation limit. Constraints (2f) and (2g) measure the timetable deviation for each leg. Constraints (2h) and (2i) stipulate that the aircraft minimum turnaround times and the train dwell times at station are satisfied, respectively. Constraints (2j) to (2r) ensure that the number of scheduled flights per time interval does not exceed the authorized runway capacity, and that the number of trains scheduled to stop at a station does not exceed its number of tracks. For instance, equation (2n) counts, for each airport, the number of flights scheduled to arrive per slot window of the day. If the arrival throughput is evaluated per 60-minute interval, as h is set to 5 minutes, we fix $w = 12$. Thus, the arrival throughput is evaluated between slot 0 and slot 11, then between slot 12 and slot 23 and so on. Remark that the summation counter τ is always a valid index since w is defined such that $\frac{N_{\text{slots}}}{w}$ is integer. Constraints (2o) are similarly defined for airport departure runway throughput evaluation. Constraints (2s) to (2w) are classical linearization constraints to account for the convex piecewise-linear cost function c_θ. Constraints (2x) and (2y) guarantee air-air connections for passengers, while constraints (2z) to (2aa) ensure the passenger transfer feasibility. Finally, constraints (2ab) and (2ag) specify the definition domain of the decision variables.

The bi-criterion resolution approach is presented in the following subsection.

3.3 Bi-criterion resolution approach

As a reminder, the problem involves a bi-criterion objective function. The first criterion is the passenger discomfort, defined in terms of multimodal transfer time, while the second criterion is the changes in the schedule of airlines and railway operators, both to be minimized. These two objectives are competing. Here, we prioritize the passenger criterion and the schedule deviation is considered as a secondary objective. In order to solve such *lexicographic-order* optimization problems, two solutions are generally proposed in the literature (Chankong and Haimes [1983]). The first method consists in *scalarizing the problem*, through the consideration of a weighted sum of the criteria. The second method is referred to as the *ϵ-constraint method*. This involves successively minimizing a criterion, with the additional constraint that the value of other criterion is not greater than ϵ. The advantage of such a sequential optimization process is that no weighting parameter has to be managed by the user. This is generally more robust for the final user. This is the method chosen here. In the following we denote $f_0^P = \sum_{e \in \mathcal{E}^{\text{rail,air}}} d_e c_e$, the value of passenger discomfort function for the solution of the problem P. Similarly, we denote $f_1^P = \sum_{l \in \mathcal{L}} \delta_l$ the schedule deviation of the solution for P. We also denote P_0 and P_1 the monocriterion problems of minimizing criteria f_0 and f_1, respectively (with all the constraints seen before). As explained earlier, the passenger criterion is prioritized. Hence, P_0 is solved first and the solution value $f_0^{P_0}$ is obtained. Then, P_1 is solved with the additional constraint that the passenger criterion value is not degraded. Hence, we set ϵ_0 such as $|f_0^{P_1} - f_0^{P_0}| \leq 10^{-2}$. It should be noticed that this method does not provide a global optimum since each monocriterion problem is solved sequentially.

In order to synchronize relevant connections, the demand for each transfer must be known (input data). However, these data are generally not available for several reasons. In order to fill this gap, a passenger demand instance generation is proposed and presented in the next section.

4 Multimodal demand instance generation

While airlines know their passengers itineraries within the air transportation network, and rail operators know about passenger rail connections, to the authors' best knowledge, no public information on multimodal transfers between rail and air exists. The demand, and consequently the passenger volume, remains unknown. Mobile phone data could bring quantitative insight (Marzuoli et al. [2019], Burrieza-Galán et al. [2022]), however several issues remain. Firstly, WiFi data are not precise in terms of location within the airport and cannot bring any additional information on passenger first mode. Secondly, mobile phone operators have different market penetration rates, hence data from several operators is required to measure the actual passenger volume. In addition, such data is rarely publicly available due to privacy concerns and existing regulation. In order to overcome this lack of available data, we next consider the problem of generating multimodal passenger demand based on the data available (schedules, transfer and rail shares) at each airport. We propose a generic model of this instance-generation problem. In order to simulate instances that are realistic, inherent constraints, such as transferring-passenger volume and the relevance of transfers are taken into account. Finally, in order to generate a sufficiently diverse instance set, a resolution approach using constraint programming (CP) is used.

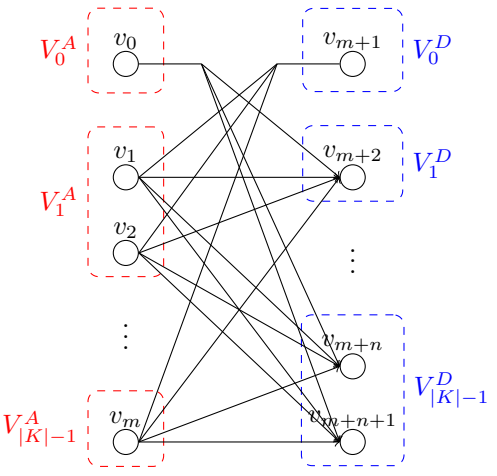

Figure 3: Graph representing a transportation station. Nodes correspond to arriving and departing legs and edges correspond to feasible transfers between them. Artificial nodes v_0 and v_{m+1} represent passengers arriving from and departing to the ground, respectively. Nodes are aggregated per means of transportation.

4.1 Passenger multimodal demand simulation model

A passenger demand instance corresponds to the volume of passengers that transfer between each leg pair, and we formulated this instance-generation problem as a routing problem within a graph. In this section, notations introduced are independent from the previous section. Notations and indices are first introduced, followed by input data, decision variables and constraints.

4.1.1 Definition of the required index sets

A station can be represented by a graph, $G = \{V, E\}$, where the vertex set, V, is partitioned into the arriving-leg vertex set, V^A, and the departing-leg vertex set, V^D, and where the set of edges, E, corresponds to feasible transfers between legs. We denote m the number of arrivals and n the number of departures. We assume that the station is served by a set of transportation modes represented by the index set K. Thus, the set of arrival vertices is further partitioned as $V^A = \bigcup_{k \in K} V_k^A$, where V_k^A is the index set of arriving legs of mode k, $k \in K$. The set of departing legs is similarly defined: $V^D = \bigcup_{k \in K} V_k^d$, where V_k^D is the index set of departing legs of mode k, $k \in K$. Finally, two artificial legs, v_0 and v_{m+1}, are added to the graph in order to account for passengers arriving from the ground, and those leaving the station, respectively. Figure 3 displays the notations introduced. Our objective is therefore to estimate the volume of passengers that transfer between two legs.

4.1.2 Input data

For each leg $v_i, i \in V$, the volume of passenger carried is denoted w_i. At the station, arriving passengers have two options. They can either transfer to another leg, that could be within the same mode or not, or leave the station. Similarly for departing legs, passengers can both arrive from another mode or directly arrive from the ground. We assume that the total volume of passengers transferring from a mode $k \in K$ to $k' \in K$ is known and denoted $W_{kk'}$. Indeed, the total volume of departing passengers can be computed as $W^{\text{out}} = \sum_{i \in V^D} w_i$. In particular, we can compute the total passenger volume leaving the station with mode k as $W_k^{\text{out}} = \sum_{i \in V_k^D} w_i$. Let $p_{kk'}$ be the share of passenger volume that transfers from mode k to k' at the station, $(k, k') \in K \times K$. We compute the total volume of passengers transferring from mode k to k' at the station, $(k, k') \in K \times K$, as follows: $W_{kk'} = p_{kk'} W_{k'}^{\text{out}}$.

For each arriving or departing leg $v_i, i \in V$, the maximum volume of transferring passenger to or from mode $k \in K$, depends on the number of feasible connections. For instance, for the last arriving flight of the day, passengers have no transferring option. We consider that they will all leave the station and the maximum passenger volume that transfers to a flight is equal to 0. We denote this maximum volume $\overline{y_{ik}}$, $i \in V$, $k \in K$. In practice, passengers may connect with a flight or a train the following day, but this will not be considered in the present study. For

each arriving leg $v_i, i \in V^A$, we define V_{ki}^D the set of departing legs of mode k with which passengers can make a connection. More precisely, V_{ki}^D is composed of legs of mode k with a different destination from v_i's origin, that are not reachable using the same transportation mode (including intramodal transfers), and with a departure time included in the interval $[\text{MCT}_\theta, \text{MACT}_\theta]$, where $\theta \in \Theta$ is the connection type involved. Similarly, for each departing leg $v_i, i \in V^D$, we define V_{ki}^A the set of arriving legs of mode k from which passengers of v_i can arrive. We also assume that passengers will choose a direct connection by train or by flight between an Origin-Destination (OD) pair if such a connection exists. Consequently, for each arriving leg $v_i, i \in V^A$, for each $k \in K$, we remove from V_{ki}^D legs departing to a destination directly connected from v_i's origin by a train or a flight. Similarly, for each departing leg $v_i, i \in V^D$, and for each $k \in K$, we remove from V_{ki}^A legs arriving from a city directly connected to v_i's destination by a train or a flight. We set for each leg $v_i, i \in V$:

$$\overline{y_{ik}} = \begin{cases} \min(w_i, \sum\limits_{j \in V_{ki}^D} w_j), & \text{if } i \in V^A, \\ \min(w_i, \sum\limits_{j \in V_{ki}^A} w_j), & \text{if } i \in V^D. \end{cases}$$

4.1.3 Decision variables

The objective consists in determining the volume of transferring passengers between each legs. For each $i \in V^A$ and $j \in V^D$, let the integer decision variable x_{ij} be the volume of passengers that transfer between leg v_i and v_j. For the sake of clarity, we also introduce for each leg $v_i, i \in V$, and for each transportation mode $k \in K$, the auxiliary integer decision variable y_{ik} that corresponds to the volume of passengers transferring from leg v_i to/from a leg of mode k.

4.1.4 Constraints

An acceptable solution must satisfy the following constraints:

$$\sum_{j \in V_k^D} x_{ij} = y_{ik} \qquad k \in K, i \in V^A, \tag{3a}$$

$$\sum_{i \in V_k^A} x_{ij} = y_{jk} \qquad k \in K, j \in V^D, \tag{3b}$$

$$\sum_{k \in K} y_{ik} = w_i \qquad i \in V, \tag{3c}$$

$$y_{ik} \leq \overline{y_{ik}} \qquad k \in K, i \in V, \tag{3d}$$

$$\sum_{i \in V_k^A} y_{ik'} = W_{kk'} \qquad (k, k') \in K \times K, \tag{3e}$$

$$\sum_{j \in V_{k'}^D} y_{jk} = W_{kk'} \qquad (k, k') \in K \times K, \tag{3f}$$

$$x_{ij} \in \{0, 1, \ldots, \min(w_i, w_j)\} \qquad i \in V^A, j \in V^D, \tag{3g}$$

$$y_{ik} \in \{0, 1, \ldots, \overline{y_{ik}}\} \qquad i \in V, k \in K. \tag{3h}$$

Constraints (3a) and (3b) correspond to classical flow constraints. Constraints (3c) ensure that the number of passengers assigned to each leg equals the passenger volume carried. Constraints (3d) stipulate that the share of transferring passengers per leg to/from each mode does not exceed the maximum authorized limit. Constraints (3e) and (3f) ensure that all passengers are assigned. Finally, constraints (3g) and (3h) specify the definition domain of the decision variables.

The resolution approach is presented in the following subsection.

4.2 Resolution approach

A multimodal passenger demand instance is a solution of the feasibility problem defined above. A first approach lies in setting a constant-objective function value, and solve the resulting optimization problem using an optimization solver. However, two issues remain. First, the constraint matrix is not *totally unimodular* (see Schrijver [1998]), implying that an integrity constraint must be included in the optimization problem, which requires the use of an mixed-integer progamming (MIP) solver, increasing the computation time. Secondly, linear-programming based

methods, such as MIP solvers, generally return solutions with saturated constraints, which in our case, will result in solutions with a high number of passengers transferring between few leg pairs and none on the other leg pairs. In order to overcome these issues, we propose to use a CP resolution approach (Rossi et al. [2006]) to address directly the feasibility problem. CP relies on a tree-search approach. At each step, a variable is selected and assigned to a value of its definition domain. The search continues while no inconsistency is found. In order to reduce the computation time, we set the choice of the next variable to be assigned using the weighted constraint algorithm (Boussemart et al. [2004]). Then, we impose the variable assignment to be randomly made in the variable definition domain, to avoid saturated constraint and increase the diversity in solutions.

This method is applied on the Western European case study. Several passenger demands are simulated for an entire week of 2019. Then, the ARTS problem is solved on these instances. A description of the case study and results obtained are presented in the following section.

5 Western Europe case study

In this section, the whole methodology presented (optimization model, resolution approach and passenger demand simulation) is tested on the case study of Western Europe. The framework of the study is detailed, followed by the passenger demand simulation results for that specific case. The ARTS problem is solved on these generated instances, results are presented in the final subsections. All the computations are performed on a laptop equipped with an AMD Ryzen 5 4500U CPU and 16 GB RAM.

5.1 Case study presentation

The multimodal network studied is composed of 18 airports: the six largest airports of France, Germany and Spain. For each day between December 2^{nd}, 2019 and December 7^{th}, 2019, all flights operated by an aircraft that stops in one of these 18 airports are considered. Eurocontrol historical flight schedules are used for the study (Eurocontrol [2023]). On average, 10,153 flights per day are considered. A particular focus is made on three airports: Paris-Charles de Gaulle airport (CDG), Frankfurt airport (FRA) and Madrid-Barajas airport (MAD). These are hub airports with several thousands of connecting passengers each day. In addition, CDG and FRA have a direct access to HSR stations: Aéroport-Charles de Gaulle 2 TGV station and Frankfurt Flughhafen Fernbahnhof. Hence, passengers arriving from a train can directly connect with a flight. On the contrary, MAD airport is not equipped with a direct HSR station. In the following, we consider connections with trains arriving at Madrid-Atocha train station. For each of these three train stations, trains scheduled to stop during the day are included in the study. For passengers

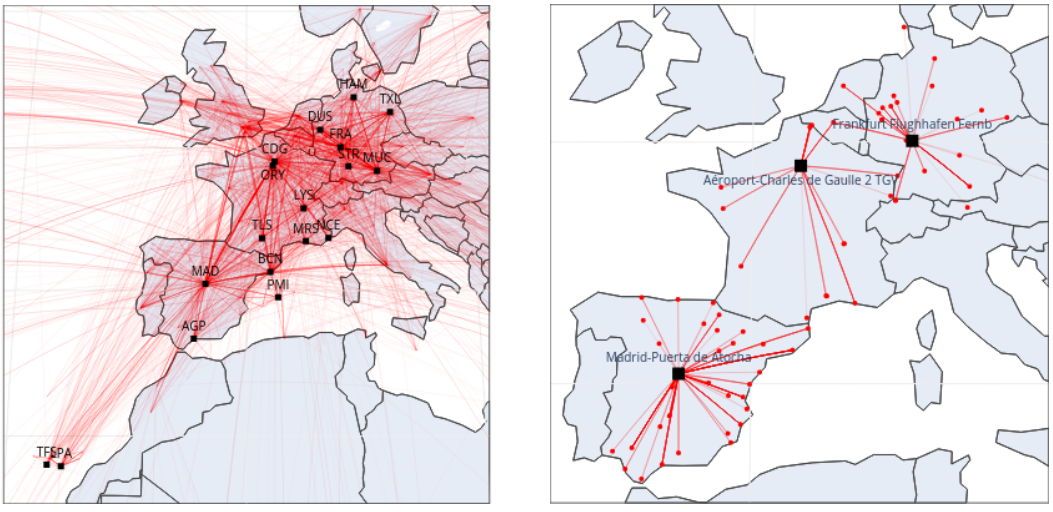

(a) Air transportation network

(b) Rail transportation network

Figure 4: Transportation networks considered. Airports and train stations are represented by black points, rail legs and flights by red lines. The width increases with the frequency of legs operated between each OD pair per day.

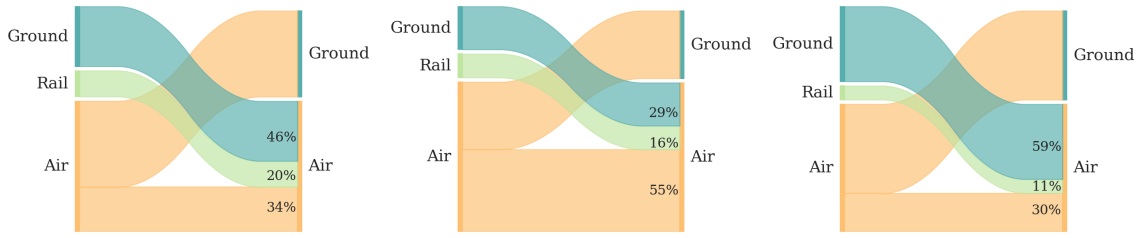

(a) CDG, $V^D_{Air} \sim 90,000$ (b) FRA, $V^D_{Air} \sim 76,000$ (c) MAD, $V^D_{Air} \sim 75,000$

Figure 5: Transfer (from left to right) volume estimation for the week starting on December 2^{nd}, 2019 for CDG, FRA and MAD airports, together with the average volume, V^D_{Air}, of departing passengers per day at the airport.

arriving at Madrid-Atocha, an additional transfer time of 45 minutes to reach the airport from the train station is added (RENFE [2022]). Train schedules are obtained after processing General Transit Feed Specification (GTFS) data, released by the French, Spanish and German railway operators: SNCF, RENFE and Deutsche Bahn (SNCF [2023], RENFE [2023], DeutscheBahn [2023]). Similarly, this leads to consider 561 rail legs per day, on average. The air transportation network and the rail transportation network are presented in Figure 4.

The ARTS problem is then tested to coordinate flights at these three hubs with their associated train stations. Note that airport *capacity* constraints are only evaluated on the 18 airports. Similarly, train station *capacity* constraints are evaluated on the three train stations presented in the case study. However, aircraft turnaround times and train stop duration constraints are taken into account at each airport and train station visited by an aircraft or a train. As an example, on December 2^{nd}, 2019, this leads to a total of 496 airports and 72 train stations.

5.2 Multimodal demand simulation results

An entire week of December 2019 is simulated. For each airport, air transfer share is collected from several previous studies (Burrieza-Galán et al. [2022], Maertens et al. [2020]). Regarding rail modal share, MAD rail share is obtained from the work of Burrieza-Galán et al. [2022]. FRA rail share data come from the airport website (Fraport [2021]). CDG rail share is estimated with the use of rail open-access data, as SNCF publishes the annual volume of rail passengers stopping at CDG-HSR station. In 2019, this CDG-HSR volume represents 20% of the annual airport passenger volume. This value is then used as an estimator for the rail-share of CDG airport. Values are summarized in Figure 5. Based on these aggregated passenger volumes, for each day between December 2^{nd}, 2019 and December 7^{th}, 2019, ten instances are generated using the method presented in Section 4. For air-air connections, we assume

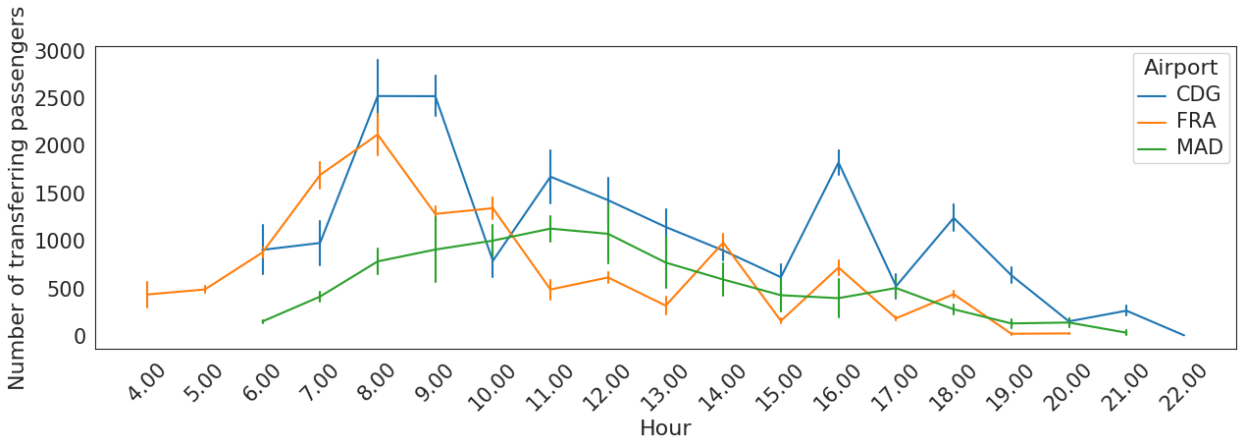

Figure 6: Average number of transferring passengers per hour for the 6 days considered. Vertical bars correspond to the standard deviation. A distinction is made between airports.

that passengers transfer only between two flights of airlines pertaining to a same alliance. The generated instances are available online (Buire [2023]). The problem is solved with the CP open-access tool Choco (Prud'homme and Fages [2022]).

On average, the algorithm takes three seconds to generate one instance. The computation time is function of the number of transferring passengers to assign. Indeed, the largest computation time occurs for FRA airport, since 71% of departing passengers arrive from another flight or from a train. Figure 6 presents the average volume of transferring passengers per hour throughout the 60 generated instances. Hours correspond to the arrival time of the train. Madrid airport has the lowest number of connections since the modal share for trains is the lowest among the three. For CDG and FRA airports, most of the connections are in the morning. Indeed, as for flight-flight connections, most of the long-range flights depart during the morning bank. Averaging over the 60 instances generated, these simulations involve more than 8,000 daily air-air connections and around 2,400 daily rail-air connections. In the following section, the resolution of the ARTS problem applied to these passenger demand instances is presented.

5.3 Air-rail timetable synchronization results

In this section, the ARTS problem is solved for each of the 60 generated instances. In Europe, there is an agreement between 26 countries to abolish border controls. These countries constitute the Schengen area. This implies a reduction in the airport processing time for flights operated within these countries. These flights are referred to as Schengen flights. Flights with a destination outside the Schengen area are referred to as non-Schengen flights. Hence, we define $\Theta = \{\text{Schengen}, \text{non-Schengen}\}$ the connection type sets considered, where "Schengen" correspond to train-flight connections with a flight destination within the Schengen area, and "non-Schengen" to train-flight connections with a flight destination outside the Schengen area. Values of each parameter defined in Section 3 are summarized in Table 1. We made the assumption that the passenger discomfort cost-function is equal to 1 when transfer time equal MCT_θ or MACT_θ, $\theta \in \Theta$. These values can be tuned by the final user. Values of MCT_θ, MACT_θ,

Table 1: Parameters values (input data) used in the instances; $\delta^{\max}$, Δ, MCT_θ, $\underline{t_\theta}$, $\overline{t_\theta}$ and MACT_θ are in minutes.

Passenger cost-function parameters									$\delta^{\max}$	Δ
θ	MCT_θ	$\underline{t_\theta}$	$\overline{t_\theta}$	MACT_θ	$c_{\theta,1}$	$b_{\theta,1}$	$c_{\theta,2}$	$b_{\theta,2}$		
Schengen	45	80	100	270	$\frac{1}{\text{MCT}_\theta - \underline{t_\theta}}$	$\frac{-\underline{t_\theta}}{\text{MCT}_\theta - \underline{t_\theta}}$	$\frac{1}{\text{MACT}_\theta - \overline{t_\theta}}$	$\frac{-\overline{t_\theta}}{\text{MACT}_\theta - \overline{t_\theta}}$	30	15
non-Schengen	60	110	130	300						

$\underline{t_\theta}$ and $\overline{t_\theta}$ are chosen according to several studies (Dennis [1994], Burghouwt and de Wit [2005], Danesi [2006]), but they can be tuned by the final user depending on the airport considered. For each airport, the maximum runway capacities are evaluated according to the number of flights scheduled to depart and arrive for each 10-minute interval and 60-minute interval of the day, in the initial planning. Similarly, the initial number of trains at a train station is computed from the initial schedule.

In addition to the initial train and flight schedules, three scenario are tested. The first scenario, S1, assumes that railway operators adapt their schedules to given flight schedules. Only changes to the train schedules are authorized in the optimization process. Similarly, scenario S2 corresponds to the case of airlines adapting their schedules to given train schedules. Only changes in the flight schedules are authorized. Finally, scenario S3 allows one to apply changes in both train and flight schedules. This last scenario corresponds to a bilateral agreement between rail and air operators to improve the passenger connection quality. The resolution of our optimization problem formulation

Table 2: Average computation time, μ, in seconds, and the associated standard deviation, σ, for the 60 instances considered, for the two monocriterion subproblems P0 and P1.

	P0 (passenger discomfort)			P1 (schedule deviation)			Total
Scenario	μ (s)	σ (s)	MIPGap (%)	μ (s)	σ (s)	MIPGap (%)	μ (s)
S1	0.8	0.1	0.1	0.9	0.2	0.1	1.7
S2	357.2	73.3	0.3	790.3	303.1	0.9	660.3
S3	289.1	46.7	0.8	1,386.5	344.2	1.1	1,675.6

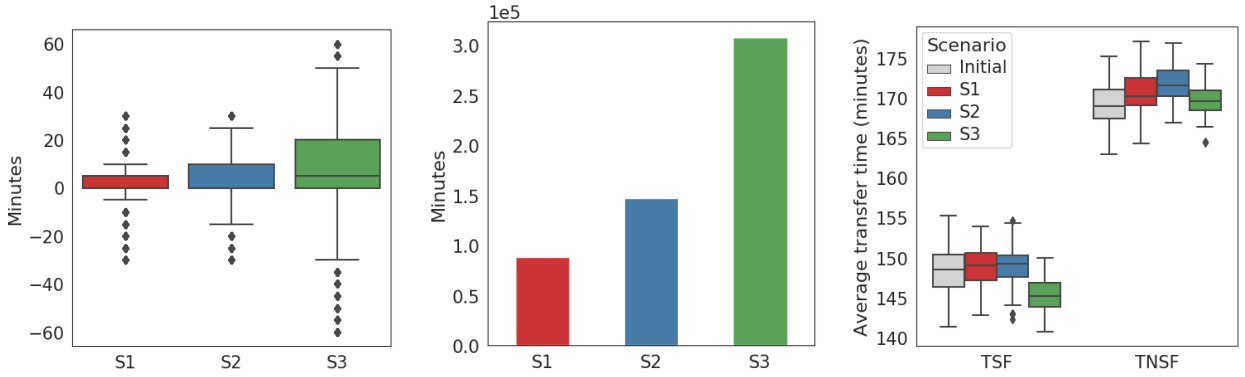

(a) Total number of minutes gained per connection, per simulation.

(b) Total minutes gained per day, on average.

(c) Average transfer time per simulation.

Figure 7: Distribution of minutes gained per connection in each scenario (7a), total passenger minutes gained (7b) on average, and average transfer time (7c) for scenario S1, S2 and S3.

is made using the MIP solver Gurobi, version 9.1.2 (Gurobi Optimization, LLC [2023]). Computation times for each scenario are presented in Table 2. A time limit of 30 minutes is set for the resolution of each monocriterion subproblem P0 (passenger discomfort) and P1 (schedule deviation). The total computation time is around 2 seconds, 10 and 29 minutes on average for scenarios S1, S2 and S3, respectively. As the tool is assumed to be run several week in advance, the computation time is acceptable for practitioners. Results obtained for each individual scenario are discussed in the following subsections.

5.3.1 Benefits of air-rail collaboration

Figure 7a presents the average number of minutes gained per connection in each scenario S1, S2 and S3. For passengers initially having a short connection time ($t < \underline{t_\theta}$), these minutes correspond to additional minutes in the new schedule. Conversely, for passengers with initially a long connection time ($t > \overline{t_\theta}$), these minutes correspond to a reduction in their connection time. On average, 8 minutes per connection are thereby gained when both airlines and railway operators are changing their schedules. If only the train schedule is modified, 2 minutes on average could be gained per connection, compared with 4 minutes if only the flight schedule is changed. As expected, changing both

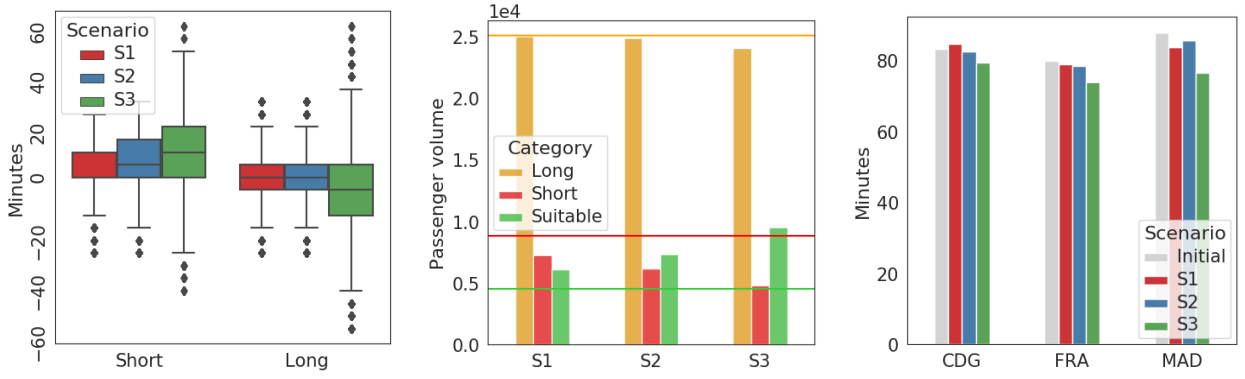

(a) Shift in minutes per connection.

(b) Passenger volume. Horizontal lines correspond to the initial planning.

(c) Average passenger waiting time.

Figure 8: Shift in connection time (8a) as a function of the initial connection category (*short* and *long*), passenger volume per connection category for each scenario (8b), and average waiting time for passengers initially experiencing *long* connection time at the three hub airports (8c).

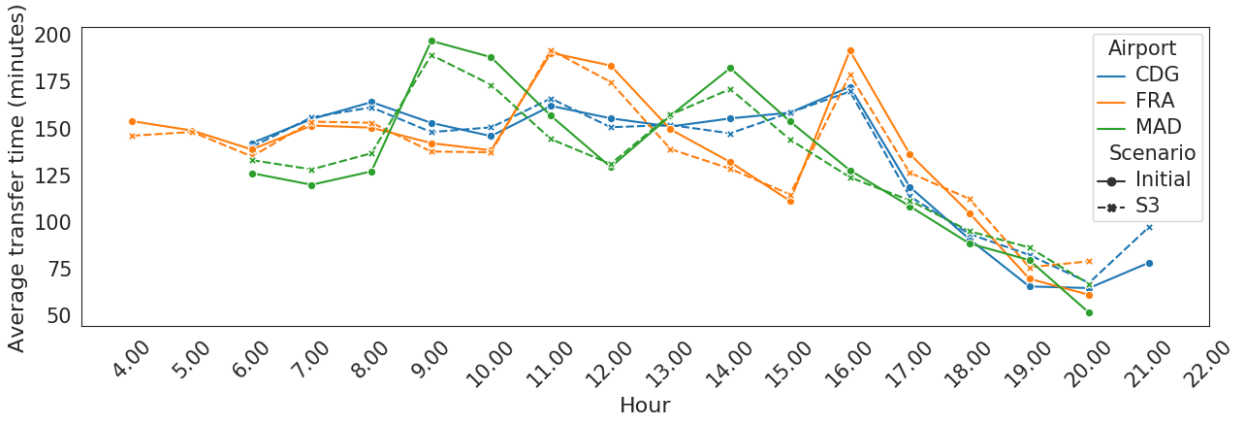

Figure 9: Train-to-Schengen-flight average transfer time, per hour for the six days considered.

rail and air schedules allows one to obtain a higher benefit for passengers, since this improves (reduce or increase) the connection time by up to one hour, compared with only 30 minutes if we authorize changes in only one mode. Moreover, 50% of transferring passengers gain more than 5 minutes per connection in scenario S3. Figure 7b displays the total number of minutes gained per day, per scenario. Scenarios S1 and S2 already improve the passenger experience by gaining around 1,700 and 2,500 hours for passengers, respectively. These hours correspond to extra waiting time or stressful tight connections for passengers. However, if both airlines and railway operators collaborate, it is more than 5,000 hours that could be thereby gained for passengers. This value is even larger than the sum of each one obtained in the unilateral scenarios. This shows that collaboration between modes brings a substantial added value for passengers. For each considered scenario, the average transfer time per simulation is displayed in Figure 7c. A distinction is made between transfers to a Schengen-destination flight (TSF) and a non-Schengen-destination flight (TNSF). In the initial planning, the average transfer times in the three considered hubs, from a train to a Schengen-flight and non-Schengen-flight are 148 minutes and 169 minutes, respectively. While S1 and S2 scenarios slightly increase the average transfer time for passengers, S3 decreases the average transfer time for TSF connections and does not change it for TNSF connection. Recall that since short connections are not robust in case of delay, their time-unit cost, $c_{\theta,1}$ is set higher than $c_{\theta,2}$, the time-unit cost of long connections (Figure 1), and the relative importance of these two time-unit costs can be set by the user. Moreover, for scenarios S1 and S2, only one transportation mode can adapt its schedule. Consequently, short connections are removed in priority. To illustrate that, Figure 8a displays the changes in minutes per connection, for each scenario, based on the initial category of the connection: *short* ($t < \underline{t_\theta}$) or *long* ($t > \overline{t_\theta}$). One can observe that for scenarios S1 and S2, short connections are lengthened, while long connections are sometimes not improved, at the benefit of passengers having short connections. In addition, scenario S2 reduces the number of short connections more than S1 does, since the number of flights is significantly higher than the number of trains, increasing thereby the magnitude of the change. Regarding scenario S3, in which both flight and train schedules are optimized, short connections are lengthened, while long connections are shortened, decreasing the average transfer time. Figure 8b displays the average volume of passenger experiencing *short*, *suitable* and *long* connections, for each tested scenario. Scenario S3 accommodates almost 25% of intermodal passengers with an ideal connection time. This value is twice that of the initial planning. However, note that, generally, long connections are proposed to passengers. Figure 8c displays the average waiting time in minutes for passengers with long connections at the three considered hubs. More precisely, these minutes correspond to extra minutes (above the ideal connection time, $\overline{t_\theta}$). On average, rail passengers wait more than one hour for their flights. Scenario S3 reduces the average waiting time of passengers by 4, 6 and 9 minutes at CDG, FRA and MAD, respectively. These values are obtained considering passengers initially having long connection times. However, as shown in Figure 8b, the number of passengers with long connections is reduced by 4%.

Figure 9 displays the average transfer time for passengers arriving by train within a given hour to a Schengen flight. For instance, on average, passengers arriving by train at FRA airport between 9am and 10am and connecting with a Schengen flight, wait 142 minutes, in the initial planning. After optimization, this value is decreased to 137 minutes. Depending on the arrival time of the train, the average optimized transfer time can significantly vary. Remark that from 4pm on, the average connection time per hour decreases. This can be explained by Figure 10 which displays the volume of passengers experiencing *short*, *suitable* and *long* connections across the day. One observes that, in the initial planning, evening connections are mostly *short* connections. In scenario S3, the average transfer time

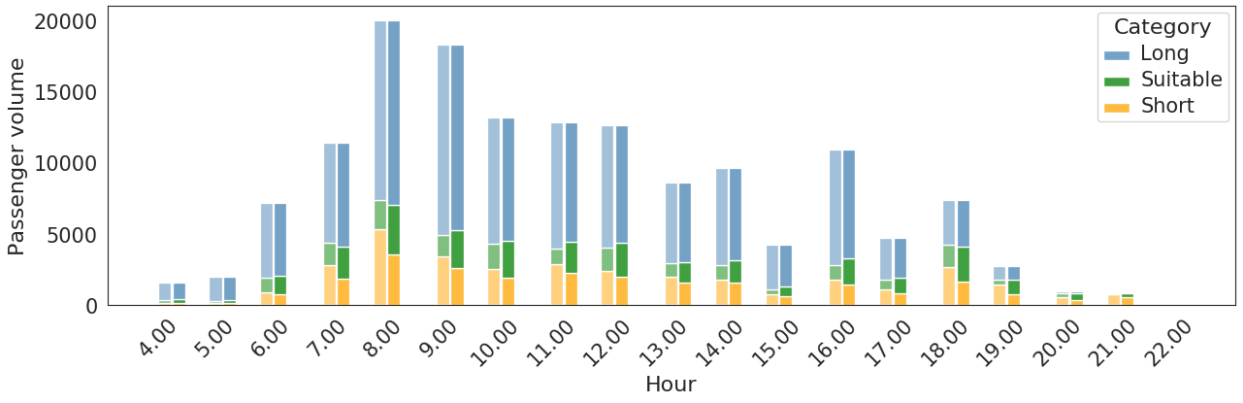

Figure 10: Distribution of connection time per category (short, suitable or long) across the day, for each hour of the day. Transparency bars (on the left) correspond to the initial planning, opaque bars (on the right), to the optimized planning with scenario S3.

is increased at the end of the day, reducing the risk of missed connection. In addition, at each hour, the number of suitable connections is increased compared with the initial schedule. On average, the number of suitable connections for all the simulation is increased by 60%. The average transfer time for *short* and *long* connections, before and after optimization, is displayed in Figure 11. In most cases, short connections are lengthened. In particular, for CDG airport, two short connections were proposed in the initial planning. They both become suitable in scenario

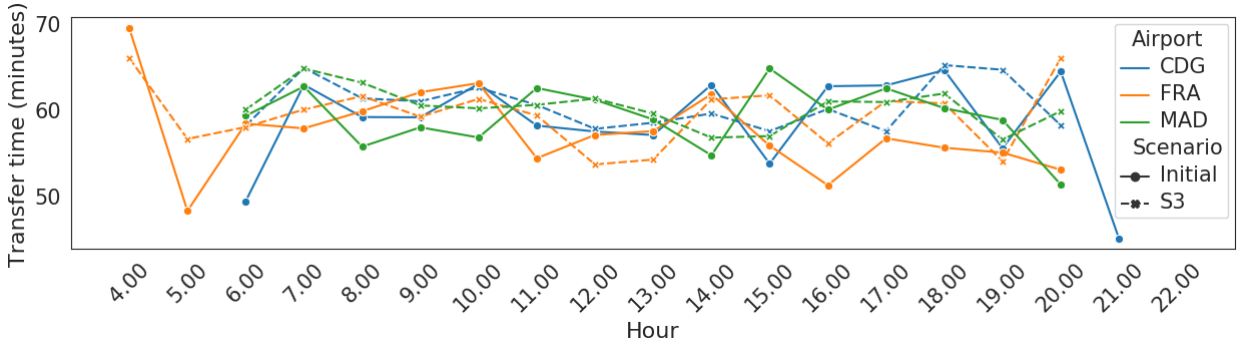

(a) Short connections

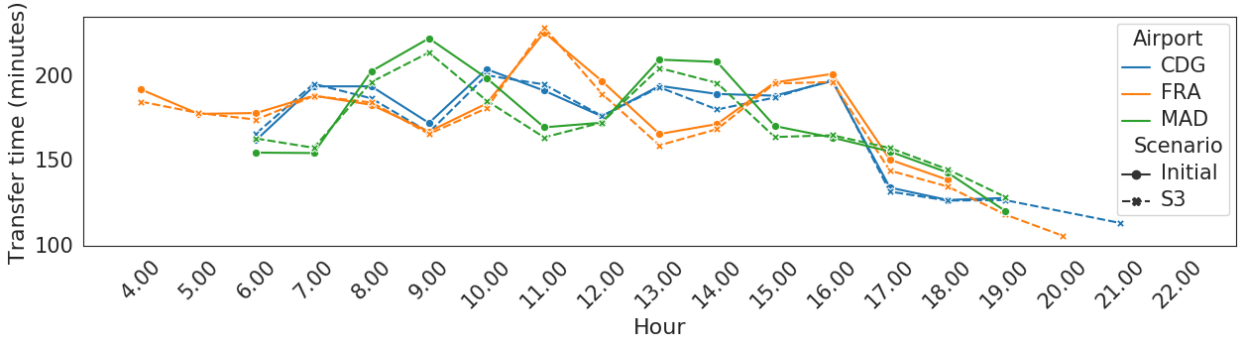

(b) Long connections

Figure 11: Average transfer time for short (11a) and long (11b) connections for TSF, per hour, for the 6 days considered.

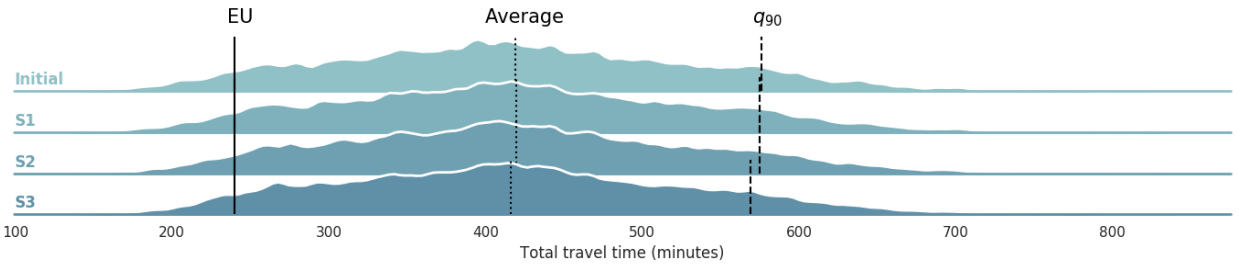

Figure 12: Schengen-destination station-to-station travel time distribution for the four scenarios (Initial, S1, S2 and S3). The EU four-hour door-to-door objective, the average door-to-door travel time, and the 90-percentile time are represented by the plain, dotted and dashed vertical lines, respectively.

S3. Regarding long connections, the average connection time is decreased by 2 minutes, on average.

Figure 10 and 11 highlight two main points. First, the number of *short* connections is significantly reduced in scenario S3, limiting the risk of missed connections for passengers. Second, for remaining *short* and *long* connections, transfer times are lengthened and shortened respectively.

Finally, Figure 12 displays the distribution of the total travel time within the Schengen area, from train origins to flight destinations, for each scenario. Note that the train departure stations are considered here, but passengers can take the train at an intermediate stop, lowering thereby the door-to-door travel time. Nevertheless, results show that the average door-to-door travel time is slightly reduced for passengers. In addition, 90% of the door-to-door travel times are below 569 minutes for scenario S3, compared with 576 minutes in the initial scenario. The following section presents the impact of optimizing air-rail timetables on transportation schedules.

5.3.2 Operator costs

The average share of legs shifted, over all 60 instances, for each scenario S1, S2 and S3, is presented in Figure 13a. A distinction is made between trains and flights. While more than 55% of trains are deviated from their initial schedules in the unilateral scenario S1, and 62% in the bilateral scenario S3, only 13% of the flights are affected by a change in both the unilateral scenario S2 and bilateral scenario S3. Note however, that only the trains stopping at the three train stations considered are counted, while all aircraft stopping at the 18 considered airports are taken into account. Thus, in reality, the proportion of trains shifted is smaller. A higher number of trains is deviated from its initial schedule in scenario S3 compared with S1. One could have expected that allowing changes in both flight and train schedules would reduce the number of legs to change. One hypothesis to explain this is that the change in flight schedule opens a wider range of possibility, as the number of trains subject to a rescheduling is much lower than the number of flights. Hence, in S1, changes in train schedule are determined by the initial flight schedule

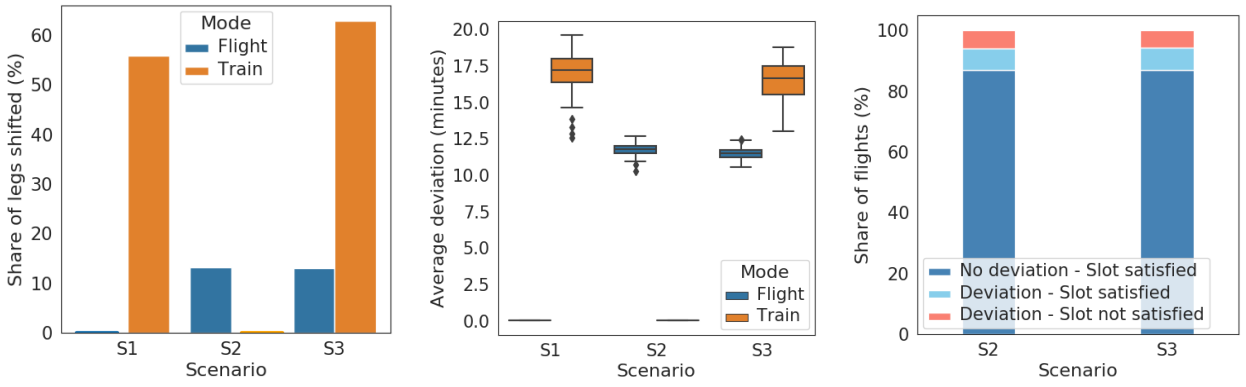

(a) Average share of legs (trains and flights) shifted.

(b) Average deviation (in minutes) per leg.

(c) Aircraft volume deviation and slot satisfaction.

Figure 13: Impact on schedules for all 60 instances.

and airport congestion. Wide changes in the train schedule are not needed since connection quality improvement is limited. However, in S3, the flight schedule can be changed as well. Ideal connection time can be reached, maybe at the cost of moving more trains than in S1. Regarding flights, approximately the same volume is changed in both scenario S2 ans S3. The average deviation (in minutes) per leg for each scenario is presented in Figure 13b. Note

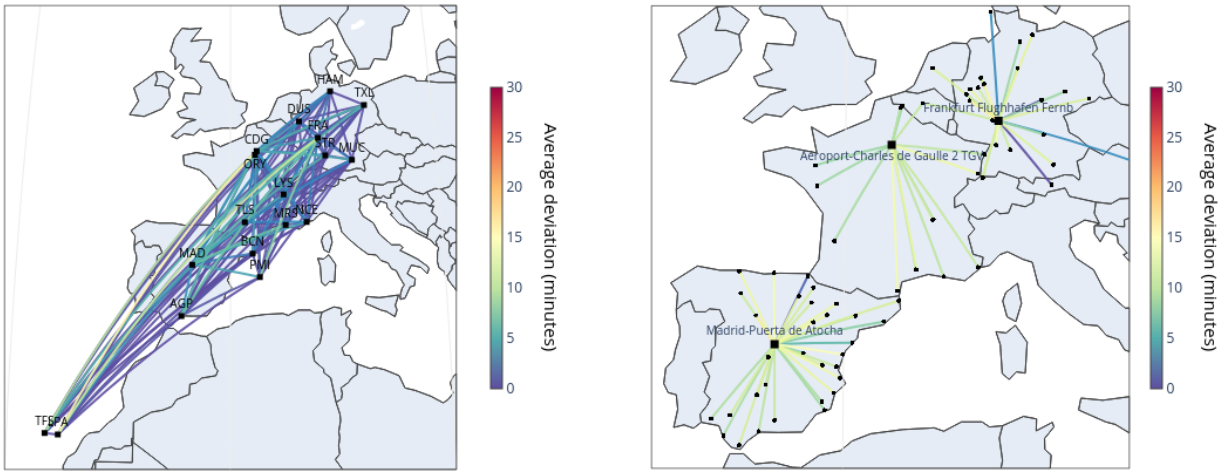

(a) Flights

(b) Trains

Figure 14: Average train and flight schedule deviations per OD pair, for scenario S3, over 60 instances.

that the average deviation is computed only among deviated legs. In both S2 and S3 scenarios, flights are shifted by 11 minutes from their initial schedule, on average. This value falls to 2 minutes if all aircraft (deviated or not) are considered. Regarding trains, they are modified from 17 to 16.4 minutes between scenarios S1 and S3. Hence, even if the number of deviated legs is increased, on average the range of the deviation decreases when both air and rail operators agree to change their schedules. Finally, Figure 13c displays the number of aircraft that satisfy their initial slots. As a reminder, a slot is satisfied if the aircraft takes off between -5 minutes and +10 minutes around its initial scheduled time. Among the total flight volume, only 13% is affected by a schedule change after optimization. In scenario S2, 54% of deviated flights still satisfy their initial slot departure time, for 56% in scenario S3. These values correspond to 6% and 5.7% of the entire flight volume, respectively, impacted by a change or not. As a result, in scenario S3, the average leg deviation is reduced with a higher gain for passengers, compared with scenarios S1 and S2. These results show that a bilateral collaboration between air and rail could benefit both transportation operators and passengers.

Figure 14 displays the average deviation over 60 instances per OD pairs for both flights and trains for scenario S3. For the sake of clarity, only flights between the 18 airports considered are displayed. Within the considered airport network, changes in schedule are, on average, below 15 minutes. The most impacted OD flight pairs are FRA-Gran Canaria airport and CDG-Gran Canaria airports. Regarding train schedules, the less coordinated legs are MAD-Valladoid for Spain, Fraknfurt-Köln for Germany and CDG-Perpignan in France.

6 Conclusion

This paper introduces an MILP formulation of the air-rail timetable synchronization problem at network level. In order to assess the benefit of air-rail collaboration, we simulated a passenger multi-modal demand based on real data for six days of December 2019, on three European airport hubs: Paris-Charles de Gaulle, Frankfurt and Madrid-Barajas airports. For each day, ten demand simulations are performed. In order to generate realistic benchmark instances, we proposed a feasibility problem, solved using constraint programming. This yields 60 instances that we made publicly available for comparison purposes. The air-rail timetable synchronization aims at providing smooth connections for passengers transferring from a train to a flight. Three scenarios are proposed, in which each operator (airlines, railway companies) agrees to change its schedule or not. Results show first that a collaboration between rail and air could yield a gain of 8 minutes per connection for passengers, on average. In addition, the number of short connections is decreased by 25%, reducing the risk of missed connections. At the same time, initially long connections are shortened, reducing the waiting time of passengers at airports. Finally, a higher benefit for both

transportation operators and passengers is obtained when air and rail transportation agree to change their schedule. Indeed, allowing changes in both schedules could reduce the average deviation from each initial schedule. In addition, a larger number of flights satisfy their initial slot departure time.

Several avenues for future work are under consideration. First, the robustness of the new schedule could be assessed against several delay patterns. Indeed, delays may severely impact the smoothness of a door-to-door journey, especially in case of missed connections. A future track of research could then consist in measuring how many passengers could avoid a missed connection with the new schedule. Then, the set of re-accommodation options for passengers in case of missed connections could be included in the optimization model. Indeed, missing a connection with a flight operated several times a day is less critical than with a daily flight. Furthermore, although such a bi-level optimization approach is not global, it allows one to obtain good results in a reasonable amount of time. A fully global optimization method could be investigated for addressing this issue. Finally, schedule elasticity should be considered since changing train or flight departure times is likely to change the demand.

Acknowlegments

We thank Dr. Nicolas Barnier (ENAC, Université de Toulouse) for his useful help in constraint programming. Authors also thank France Aviation Civile Services for providing air passengers data volume.

This document/R&D product has been created with or contains elements of ATM Datasets made available by EUROCONTROL. (©2020, EUROCONTROL). EUROCONTROL does not necessarily support and/or endorse the conclusion of this document/R&D product. EUROCONTROL shall not be liable for any direct, indirect, incidental or consequential damages arising out of or in connection with this document/product and/or underlying the ATM Datasets.

This project has received funding from the SESAR Joint Undertaking under grant agreement No 893209 under European Union's Horizon 2020 research and innovation programme.

References

F. Boussemart, F. Hemery, C. Lecoutre, and L. Saïs. Boosting systematic search by weighting constraints. In *ECAI*, volume 16, page 146, 2004.

J. Bueno, J. Burrieza, O. García Cantú, C. Livingston, M. Balac, G. Scozzaro, and C. Buire. Transit final project results report. `http://www.nommon-files.es/transit/TRANSIT-D1.3_Final_Project_Results_Report_v01.00.00.pdf`, 2022.

C. Buire. Air-Rail Passenger Demand Instances. `https://doi.org/10.57745/5WB9KG`, 2023.

C. Buire, D. Delahaye, A. Marzuoli, E. Feron, and M. Mongeau. Air-rail timetable synchronization for a seamless passenger journey. In *Proceedings of 2022 International Workshop on ATM/CNS*, pages 79–86. Electronic Navigation Research Institute, 2022.

G. Burghouwt and J. de Wit. Temporal configurations of European airline networks. *Journal of Air Transport Management*, 11(3):185–198, 2005.

G. Burghouwt and R. Redondi. Connectivity in air transport networks: An assessment of models and applications. *Journal of Transport Economics and Policy (JTEP)*, 47(1):35–53, 2013.

J. Burrieza-Galán, R. Jordá, A. Gregg, P. Ruiz, R. Rodríguez, M. Sala, J. Torres, P. García-Albertos, O. Cantú Ros, and R. Herranz. A methodology for understanding passenger flows combining mobile phone records and airport surveys: Application to Madrid-Barajas airport after the COVID-19 outbreak. *Journal of Air Transport Management*, 100:102163, 2022. ISSN 0969-6997. doi: https://doi.org/10.1016/j.jairtraman.2021.102163.

V. Chankong and Y. Y. Haimes. Optimization-based methods for multiobjective decision-making-an overview. *Large Scale Systems In Information And Decision Technologies*, 5(1):1–33, 1983.

P. Chiambaretto, C. Baudelaire, and T. Lavril. Measuring the willingness-to-pay of air-rail intermodal passengers. *Journal of Air Transport Management*, 26:50–54, 2013.

R. R. Clewlow, J. M. Sussman, and H. Balakrishnan. Interaction of high-speed rail and aviation: Exploring air–rail connectivity. *Transportation Research Record*, 2266(1):1–10, 2012.

Cohor. Aéroport Paris-Charles de Gaulle. https://www.cohor.org/aeroport-paris-charles-de-gaulle-cdg/, 2023. Visited January 2023.

A. Danesi. Measuring airline hub timetable co-ordination and connectivity: Definition of a new index and application to a sample of European hubs. *European Transport*, (34):54–74, 2006.

N. Dennis. Airline hub operations in Europe. *Journal of Transport Geography*, 2(4):219–233, 1994.

DeutscheBahn. Open data portal. https://data.deutschebahn.com/, 2023.

T. D'Alfonso, C. Jiang, and V. Bracaglia. Would competition between air transport and high-speed rail benefit environment and social welfare? *Transportation Research Part B: Methodological*, 74:118–137, 2015.

T. D'Alfonso, C. Jiang, and V. Bracaglia. Air transport and high-speed rail competition: Environmental implications and mitigation strategies. *Transportation Research Part A: Policy and Practice*, 92:261–276, 2016.

Eurocontrol. Aviation Data for Research. https://www.eurocontrol.int/dashboard/rnd-data-archive, 2023.

European Commission. Flightpath 2050. Europe's vision for aviation. Report of the high-level group on aviation research, 2011a.

European Commission. White paper. Roadmap to a single European transport area – towards a competitive and resource efficient transport system, 2011b.

Fluko. Airport capacity parameters. https://fluko.org/en/flughaefen/flughafen-kapazitaets-parameter/, 2023. Visited January 2023.

Fraport. Passengers at Frankfurt airport. https://www.fraport.com/en/newsroom/frafacts.html, 2021.

M. Givoni and D. Banister. Airline and railway integration. *Transport Policy*, 13(5):386–397, 2006.

Gurobi Optimization, LLC. Gurobi Optimizer Reference Manual, 2023. URL https://www.gurobi.com.

M. Janic. Assessing some social and environmental effects of transforming an airport into a real multimodal transport node. *Transportation Research Part D: Transport and Environment*, 16(2):137–149, 2011.

L. N. Jansen, M. B. Pedersen, and O. A. Nielsen. Minimizing passenger transfer times in public transport timetables. In *7th Conference of the Hong Kong Society for Transportation Studies, Transportation in the information age, Hong Kong*, pages 229–239, 2002.

C. Jiang and A. Zhang. Effects of high-speed rail and airline cooperation under hub airport capacity constraint. *Transportation Research Part B: Methodological*, 60:33–49, 2014.

Y. Jiang, S. Chen, W. An, L. Hu, Y. Li, and J. Liu. Demand-driven train timetabling for air and intercity high-speed rail synchronization service. *Transportation Letters*, pages 1–15, 2022.

Y. Ke, L. Nie, C. Liebchen, W. Yuan, and X. Wu. Improving synchronization in an air and high-speed rail integration service via adjusting a rail timetable: A real-world case study in china. *Journal of Advanced Transportation*, 2020, 2020.

P. Knoppers and T. Muller. Optimized transfer opportunities in public transport. *Transportation Science*, 29(1): 101–105, 1995.

S. Maertens, W. Grimme, and S. Bingemer. The development of transfer passenger volumes and shares at airport and world region levels. *Transportation Research Procedia*, 51:171–178, 2020.

A. Marzuoli, E. Boidot, E. Feron, and A. Srivastava. Implementing and validating air passenger–centric metrics using mobile phone data. *Journal of Aerospace Information Systems*, 16(4):132–147, 2019.

K. Nachtigall and S. Voget. A genetic algorithm approach to periodic railway synchronization. *Computers & Operations Research*, 23(5):453–463, 1996.

A. Paul. Modelling and assessing the role of air transport in an integrated, intermodal transport system. https://modus-project.eu/, 2020.

C. Prud'homme and J.-G. Fages. Choco-solver: A java library for constraint programming. *Journal of Open Source Software*, 7(78):4708, 2022. doi: 10.21105/joss.04708. URL `https://doi.org/10.21105/joss.04708`.

RENFE. Línea c-1 RENFE cercanías de Madrid. `https://www.redtransporte.com/madrid/cercanias-renfe/linea-c-1.html`, 2022.

RENFE. Renfe Data. `https://data.renfe.com/dataset?res_format=GTFS`, 2023.

F. Rossi, P. Van Beek, and T. Walsh. *Handbook of constraint programming.* Elsevier, 2006.

A. Schrijver. *Theory of linear and integer programming.* John Wiley & Sons, 1998.

SNCF. Horaire des TGV. `https://ressources.data.sncf.com/explore/dataset/horaires-des-train-voyages-tgvinouiouigo/table/`, 2023.

P. Vansteenwegen and D. Van Oudheusden. Developing railway timetables which guarantee a better service. *European Journal of Operational Research*, 173(1):337–350, 2006.

J. Veldhuis. The competitive position of airline networks. *Journal of Air Transport Management*, 3(4):181–188, 1997.

W. Xia and A. Zhang. Air and high-speed rail transport integration on profits and welfare: Effects of air-rail connecting time. *Journal of Air Transport Management*, 65:181–190, 2017.